IJCPE
Iraqi Journal of Chemical and Petroleum Engineering

Iraqi Journal of Chemical and Petroleum Engineering
Vol.17 No.2 (June 2016) 69-77
ISSN: 1997-4884

University of Baghdad
College of Engineering

CFD Simulation of Air Flow Patterns in a Spray Dryer Fitted With a Rotary Disk

Saad Nahi Saleh and Laith Amjad Hameed
Tikrit University, College of Engineering, Chemical Engineering Department
Tikrit, Salah el-Din, Iraq

Abstract

The air flow pattern in a co-current pilot plant spray dryer fitted with a rotary disk atomizer was determined experimentally and modelled numerically using Computational Fluid Dynamics (CFD) (ANSYS Fluent) software. The CFD simulation used a three dimensions system, Reynolds-Average Navier-Stokes equations (RANS), closed via the RNG k −ε turbulence model. Measurements were carried out at a rotation of the atomizer (3000 rpm) and when there is no rotation using a drying air at 25 ^{o}C and air velocity at the inlet of 5 m/s without swirl. The air flow pattern was predicted experimentally using cotton tufts and digital anemometer. The CFD simulation predicted a downward central flowing air core surrounded by a slow recirculation zones near the walls for both conditions. Analysis of CFD simulation revealed that rotation of atomizer resulted in a swirling motion of the central air core. Simulations results were in good agreement with experimental data.

Key Words: CFD, Spray, Rotary, Dryer, Simulation.

Introduction

Spray drying is a transformation process of a solution into a dried form by spraying it into a hot drying medium. This drying technique is common to many industries for the production of chemical, foodstuffs, detergents, pharmaceuticals and cosmetics [1]. The dried product can be in the form of powders, granules or agglomerates depending upon the chemical and physical properties of the feed, design of the dryer and final desired properties for product [2].

One of the most important phenomena which influences on the operation of the spray dryer is air flow pattern within the dryer. Air flow has effects on droplets trajectories, residence time distribution of droplets and deposition of the droplets on the wall [3, 4]. Therefore an accurate knowledge of the air flow pattern inside the spray dryer will help to operate the dryer at conditions that produce powders with desired equality.

Numerous numerical studies have been published for analysis of the air flow pattern in the spray dryer[5-7]. The Computational Fluid Dynamics (CFD) simulation has proven to be a valuable tool in understanding and analyzing of the air flow patterns within spray dryers [8].

The steady state air flow pattern was investigated numerically by solving Navier-Stockes equations to predict the motion of air in a spray dryer [9, 10]

A central flowing jet with a recirculation zone near the wall have been captured in a co-current spray dryer using CFD simulations [11, 12]. It was found that the simulation of the spray dryer fitted with a rotating atomizer yielded a relatively symmetrical air flow pattern [13].

The aim of this work is to predict air flow pattern experimentally and investigate numerically the behavior of air flow inside the spray dryer fitted with a rotary atomizer at a case of no solution was sprayed.

Experimental Work

The tests were conducted in a pilot plant spray dryer with total product discharge which is shown in Fig. (1). It is a co-current dryer with an internal diameter of 0.80 m, a cylindrical

Fig. 1, Pilot plant spray dryer.

Section height of 1.0 m and a conical section height of 0.69m [14]. At the top of the dryer, a rotary disk atomizer of 6 cm diameter is fitted and air enters the dryer via an annulus inlet opening (Fig. 2). The dryer main air inlet has a zero swirl condition with the flow direction normal to the inlet. A schematic diagram of the spray dryer chamber is shown in Fig. (3).

Visualization of the air flow field in the dryer was performed experimentally by two methods:-

1- Quantitative flow prediction

Digital anemometer (0-10 m/s measuring range, 0.1 m/s accuracy, 0.01 m/s resolution) was utilized at various height and radial to give an indication of the air flow inside the dryer.

2- Qualitative flow prediction

Grid of cotton tufts was utilized to assess the flow characteristics inside the spray dryer at conditions that are with and without rotation of the disc atomizer. The cotton tufts were suspended in circles (R1, R2 and R3) locating about the axis and along three levels of lengths (C1, C2 and C3) within the dryer chamber as shown in Fig. (4).

Fig.2, rotary disk

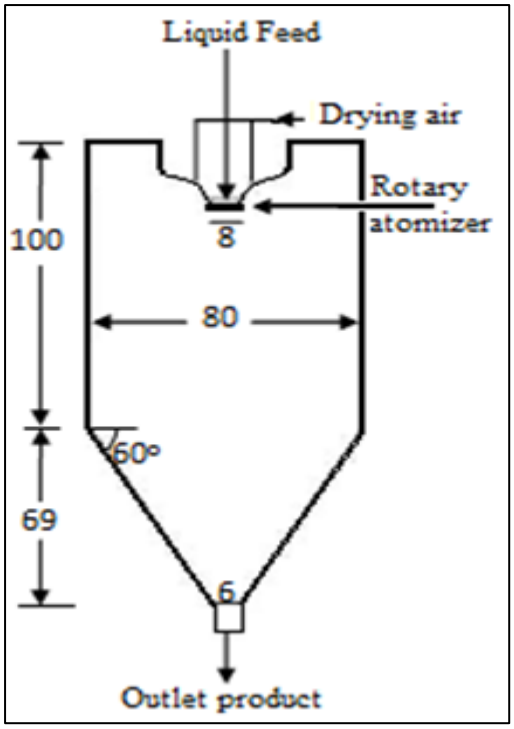

Fig. 3, Schematic diagram of dryer chamber (the dimensions in cm)

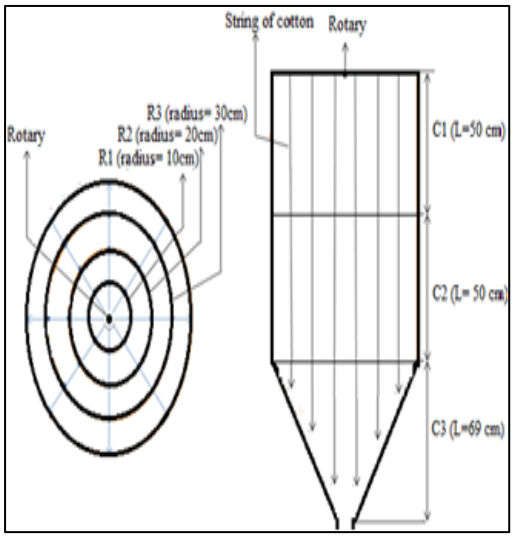

Fig. 4, the grid of cotton tufts used in the dryer chamber.

The Computational Model

In order to determine accurately the air flow features inside the spray dryer, CFD simulation was used with the software ANSYS Fluent version 15 [15] in which a three dimensional model was adapted for air flow modeling.

For modeling the air flow, the equations of continuity, momentum, turbulent kinetic energy, and dissipation rate of turbulent kinetic energy are applied.

Following are the Reynolds-Averaged Navier-Stokes equations (RANS) and the RNG k-ε model as a turbulence model:

$$\frac{\partial \rho}{\partial t} + \nabla \cdot (\rho \vec{u}) = 0 \quad \ldots (1)$$

$$\frac{\partial \rho \vec{u}}{\partial t} + \nabla \cdot (\rho \vec{u}\vec{u}) = -\nabla p + \nabla \cdot \left(\mu_{eff}\left(\nabla \vec{u} + (\nabla \vec{u})^T\right)\right) \ldots (2)$$

$$\frac{\partial \rho k}{\partial t} + \nabla \cdot (\rho k \vec{u}) = \nabla \cdot (\alpha_k \mu_{eff} \nabla k) + G_k - \rho \varepsilon \ldots (3)$$

$$\frac{\partial \rho \varepsilon}{\partial t} + \nabla \cdot (\rho \varepsilon \vec{u}) = \nabla \cdot (\alpha_\varepsilon \mu_{eff} \nabla \varepsilon) + C_1 \frac{\varepsilon}{k} G_k - C_2 \rho \frac{\varepsilon^2}{k} \ldots (4)$$

Where

$$\mu_{eff} = \mu + \mu_t \quad \text{and} \quad \mu_t = \rho C_\mu \cdot \frac{k^2}{\varepsilon}$$

The RNG k-ε model's constants C_1, C2, Cμ are 1.42, 1.68 and 0.0845 respectively [15].

Mesh generation

Geometry of the dryer chamber was created using the software GAMBIT where a three-dimensional unstructured mesh was constructed using 78216 hexahedral cells.

The surface mesh of the spray dryer chamber is shown in Fig. (5).

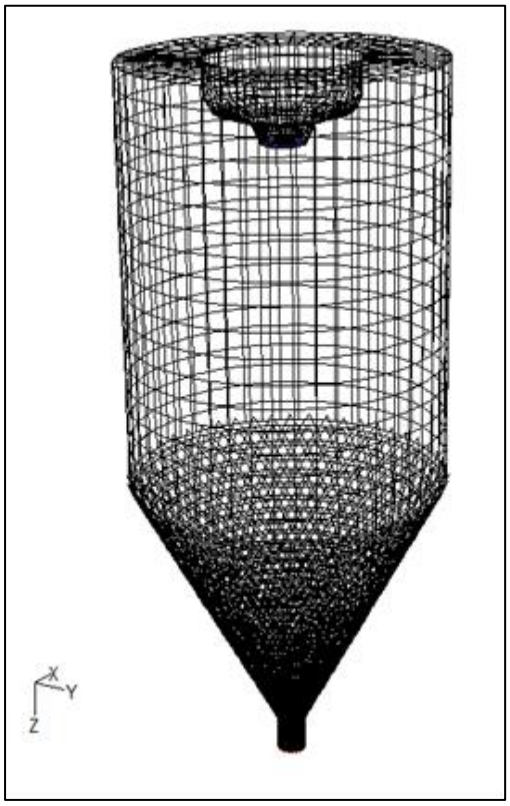

Fig. 5, Surface mesh for the dryer chamber

Boundary Conditions

The simulation was isothermal, using a drying air at 25 ^{o}C with the flow direction normal to the inlet, and no droplets were injected. The air velocity at the inlet was set to 5 m/s without swirl and the average static pressure set to zero at the outlet. The turbulent kinetic energy (k) = 0.027 m^2/s^2, rate of dissipation (ε) = 0.37 m^2/s^3.

The no slip boundary condition with standard log-law wall functions were used to solve the turbulence and air velocity near the walls.

Numerical Solution

The simulations were performed for steady state operation using ANSYS-Fluent software, which uses a finite volume discretization method to solve the fluid flow equations in the computational domain.

For the convective terms, the second-order upwind discretization scheme was used and for the pressure-velocity coupling the SIMPLE scheme was used.

The convergence criteria for the continuity, momentum, turbulent kinetic energy and rate of dissipation were specified as 1×10^{-5}.

Results and Discussion

1- Experimental Results

By observing the motion of the cotton tufts (through the sight glass mounted on the dryer chamber) at a case of atomizer stopped, it was possible to distinguish a zone of a recirculation movement of the tufts at the (R3, C2) region and an upwards motion at the tufts at the (R3, C3) region.

The velocities magnitude measured using the digital anemometer are illustrated in Fig. (6) at different vertical distance from the ceiling of the dryer.

It is shown that the velocity decrease with increasing of radial distance from the center to the wall for all vertical levels and the velocity is decreased as the air goes into the dryer further due to expanding area.

The measurements reveal that the velocity profiles near the center of the dryer are quite different at the vertical levels where a low velocity region at 10 cm level (just under the atomizer on the ceiling) is occurred because the ceiling plate blocks air flow.

By these predictions, it is clear that air flow consists of a central air core with radius about 10 cm and a slow recirculation zones around that core.

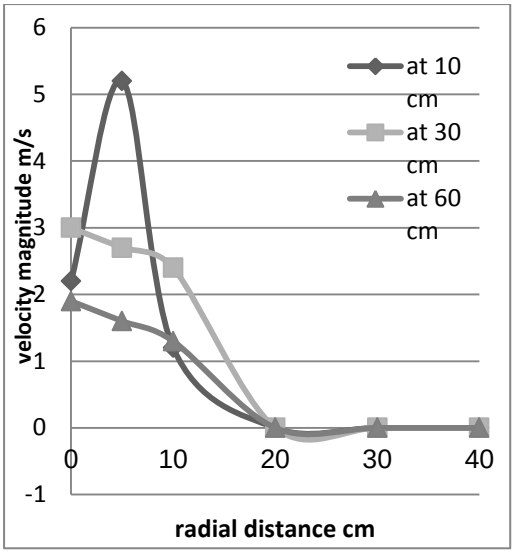

Fig. 6, Radial distribution of measured air velocity for no rotational case at different vertical levels

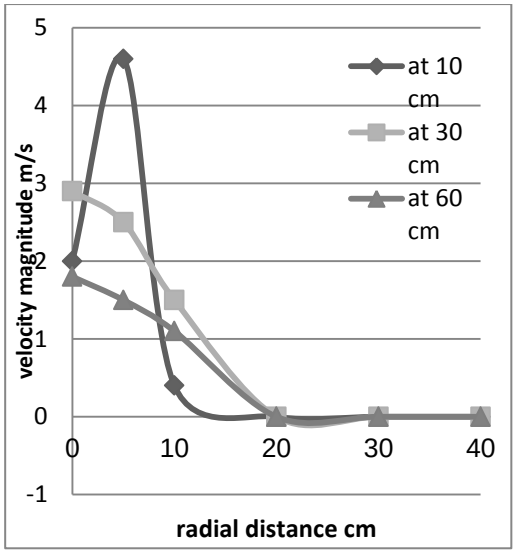

Fig. 7, Radial distribution of measured air velocity magnitude for rotational case at different vertical levels

For atomizer running case (3000 rpm), observation of the cotton tufts revealed a downward movement of air flow near the central region towards the exit in a strong clockwise swirling motion, due to the atomizer rotating in that direction.

The cotton tufts at the region (C3, R3) were moved to upward and this indicates presenting an upward recirculation zone at this region.

This motion continued to the region (C2, R3) at which a recirculation zone around the central air core was appeared. Fig (7) shows the air velocity magnitude measured using the digital anemometer at 3000 rpm rotation of atomizer. By comparing it with measured velocity of no rotation of atomizer (Fig. (6)), the main features of air flow pattern for two cases (no rotation and 3000 rpm rotation of atomizer) are almost similar where the air core of about 10 cm radius surrounding by a low velocity region is a distinct behavior in both cases.

2- Simulations Results

In this section, the analysis of air flow pattern simulated in the pilot plant spray dryer was presented.

As shown in Fig. (8) for the no rotation atomizer case, the air flow pattern inside the dryer chamber consists of the air core and low velocity zones around that core.

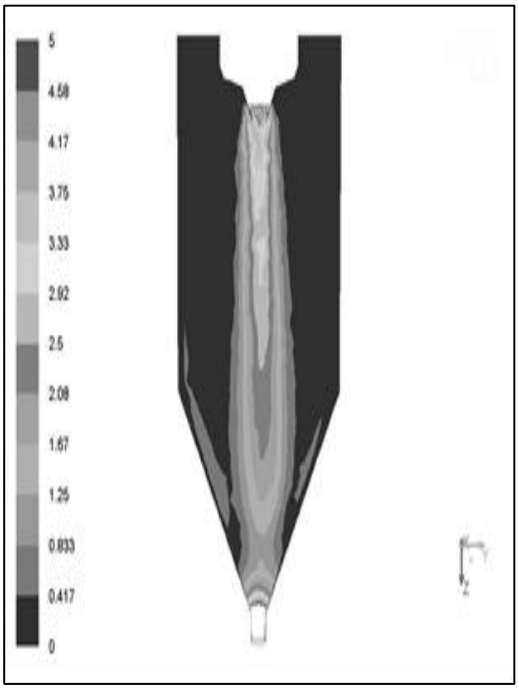

Fig. 8, Predicted air velocity magnitude (m/s) contour at without rotation of atomizer.

Fig.(9) shows the air velocity magnitude at different vertical levels where the air core broadens as it moves further downstream into the chamber.

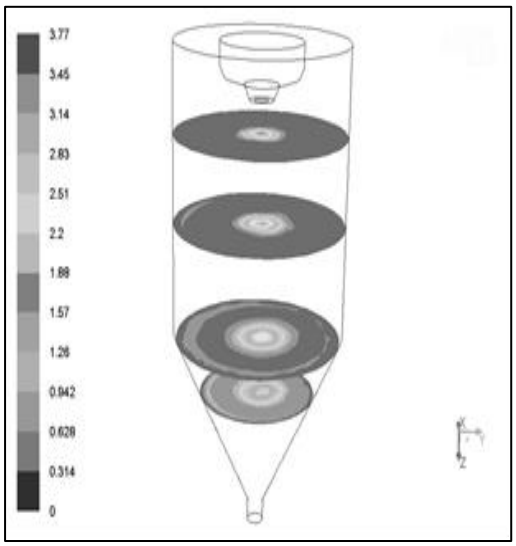

Fig. 9, Predicted air velocity magnitude (m/s) contours for no rotation case at different vertical levels.

The simulation results revealed that an air recirculation region was predicted at the cylindrical-conical interface of the dryer chamber as shown in Fig (10).

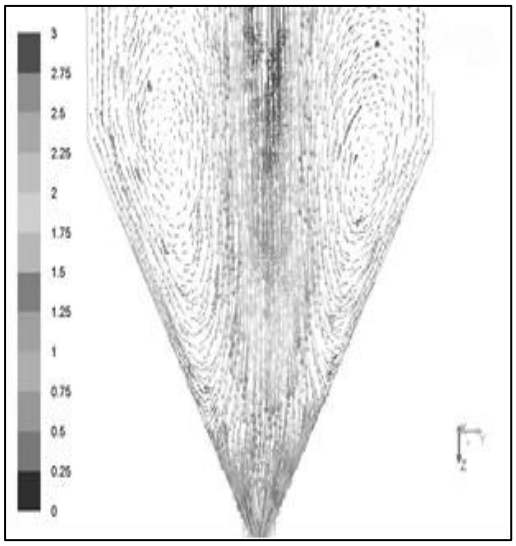

Fig. 10, Predicted air velocity magnitude (m/s) contour at conical part of dryer chamber for no rotational case

Figure (11) shows the air velocity magnitude profiles with radial distance from the center at different vertical levels (10, 30 and 60 cm from the ceiling). There is a good agreement with the experimental results with a deviation of about (8%) from experimental data. (Fig. (6)). It is noted that the predicted air core radius was about 10 cm and this is very close to that estimated from experiments.

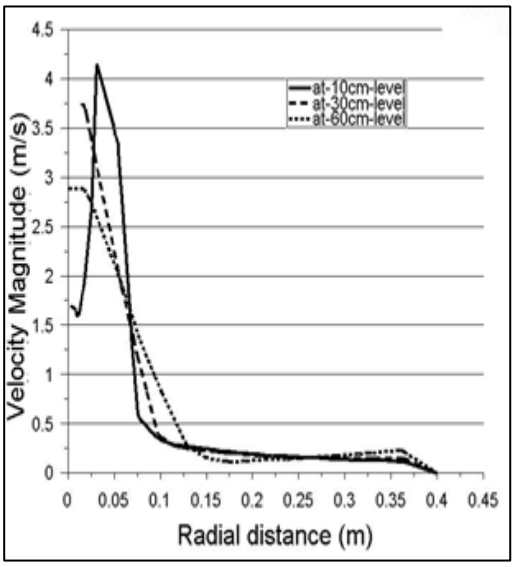

Fig. 11, Radial distribution of predicted air velocity magnitude for no rotation case at different vertical levels

Simulation results for rotational case show a swirling motion of air core where this motion continues til the conical part of the chamber as shown in Fig. (12). Thus the tangential component of velocity governs the main flow whereas the radial and axial velocities are almost negligible.

Due to the swirling motion of the air core, it is noted that the center had a lower velocities than that were at near the center of the core as shown clearly in Fig. (13) and especially at 10 cm vertical level. In comparison with no rotation atomizer, the air core have a higher velocities as it moves downward ,although the air flow structure for both cases is the same

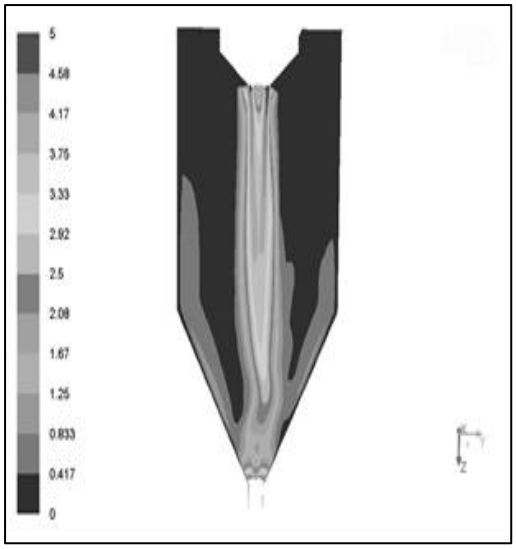

Fig. 12, Predicted air velocity magnitude (m/s) contour for rotational case

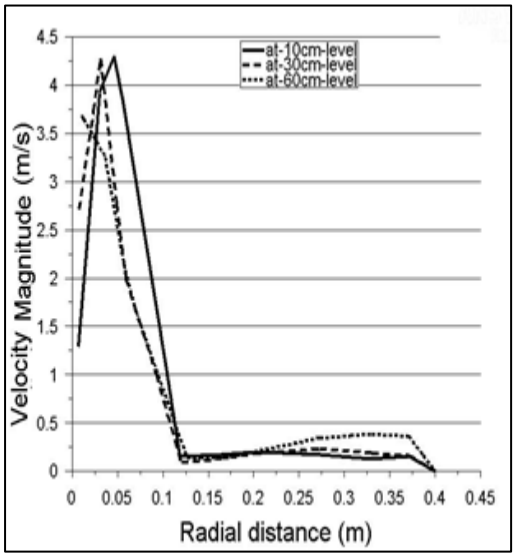

Fig. 13, Radial distribution of predicted air velocity profile for rotational case at different vertical levels

Another comparison of predicted tangential velocities for the two cases is shown in Fig. (14) in which air flow structure is asymmetrical for no rotation case (a) whereas for rotation case, the central air core is surrounded by an alternative regions of clockwise and anticlockwise flow motion and this is an acceptable agreement to what observed qualitatively by the experimental tests.

Therefore, the air flow pattern for rotational case can be described as a structure of symmetrical nature which was also captured by another model [12].

The predicted axial velocity for rotational case is shown in Fig. (15). It is seen that there is a slightly reverse flow at 10 cm level because of the rotating atomizer which pulls the air flow below the atomizer upwards. This phenomenon was called as air pumping and predicted numerically [16]. Near the wall, a revers flow is also shown and this is belonging to appearance of the air recirculation zones.

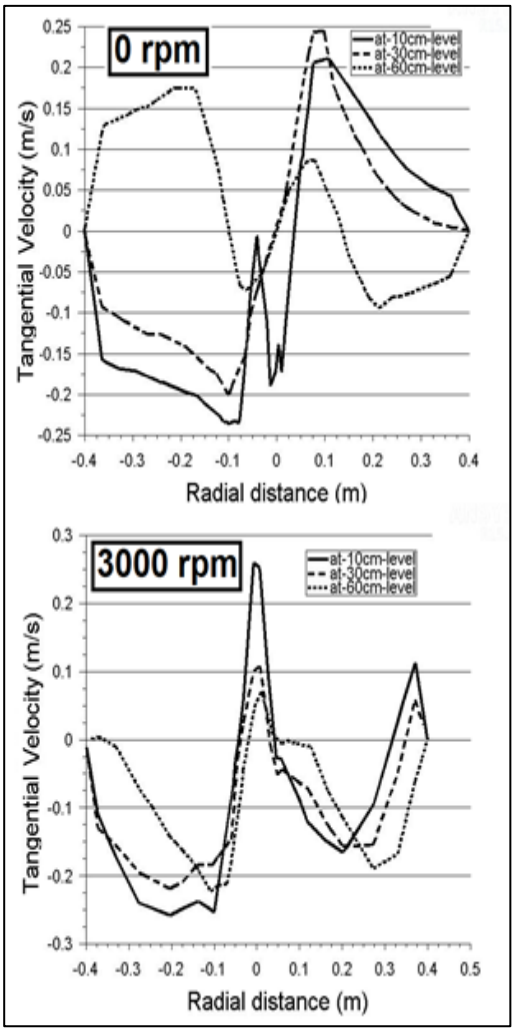

Fig. 14, Comparison of predicted tangential air velocity (m/s) contours for no rotation (a) and rotation (b) cases at different vertical levels.

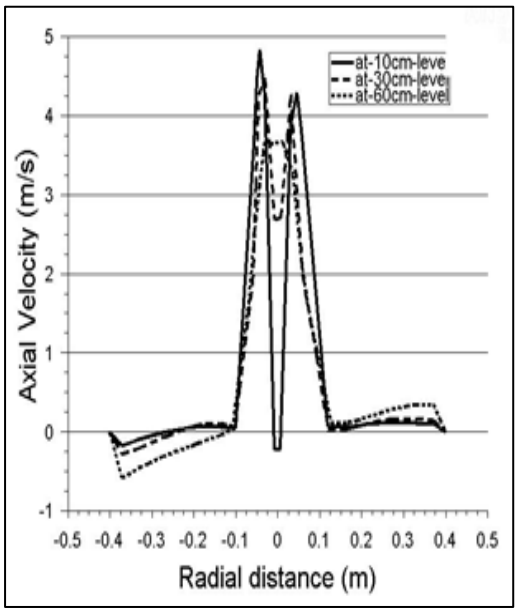

Fig. 15, Radial distribution of predicted axial velocity profile for rotation case at different vertical levels

Conclusions

The CFD simulation captured the main features of air flow structure for no rotation and rotation of atomizers cases. The air flow in both cases consists of a central air core surrounded by a low recirculation zones. In the rotation case, the rotation of atomizer resulted in a swirling motion of the central core moving downward to the chamber outlet. This rotation created an anticlockwise motion surrounding the central core. Generally the rotation of the atomizer increased the central air core velocity and caused an occurrence of the air pumping below the atomizer. The agreement between experimental observations and simulations revealed a deviation of about (8%) from experimental data.

Nomenclature

C_1, C2, Cμ	Constants
C1, C2, C3	Axial position (cm)
G_k	Generation of turbulent kinetic Energy, kg/m.s^3
K	Turbulent kinetic energy,m^2/s^2
P	Air pressure, Pa
R1, R2, R3	Radial position (cm)
U	Air velocity, m/s
T	Time, s

Greek Symbols

ε	Turbulent kinetic energy dissipation rate, m^2/s^3
μ	Viscosity, Pa.s
μ_{eff}	Effective viscosity, Pa.s
μ_t	Turbulent viscosity, Pa.s
ρ	Density, kg/m^3
α_k,α_ε	Turbulent Prandtl numbers

References

1- Masters, K., (1991), "Spray Drying Handbook", Longman Scientific and Technical: Harlow, UK.
2- Michael, J.K., (1993), "Spray drying and spray congealing of pharmaceuticals". In: Encyclopedia of pharmaceutical technology, Marcel Dekker INC, NY, Vol. 14, pp. 207.
3- Kota, K.; Langrish, T., (2007) "prediction of deposition patterns in a pilot scale spray dryer using computational fluid dynamics (CFD) simmulations", Chemical Product and Process Modeling, No.3, Vol. 2, Article 26.
4- Sadripour, M.; Rahimi, A.; Hatamipour, M.S., (2012), " Experimental study and CFD modeling of wall deposition in a spray dryer ", Drying Technology, No.6, Vol.30, pp.574.
5- Roustapour, O.R. ; Hosseinalipour, M.H. ; Ghobadian, B.; Mohaghegh, F. ; Neda, N.M., (2009), "A proposed numerical–experimental method for drying kinetics in a spray dryer", Journal of Food Engineering, Vol. 90, pp. 20.

6- Southwell, D.B.; Langrish, T.A.G, (2000), "Observations of flow patterns in a spray dryer", Drying Technology, Vol. 18,pp. 661.
7- Fletcher, D.F.; Langrish,T.A.G., (2009), "Scale-adaptive simulation (SAS) modelling of a pilot-scale spray dryer, Chemical Engineering Research and Design, Vol.87, pp.1371.
8- Oakley, D.E., (1994), "Scale-up of spray dryers with the aid of computational fluid dynamics", Drying Technology, Vol.12, No. 1, pp.217.
9- Kieviet, F.G, (1997), "Modelling Quality in Spray Drying", Ph.D. Thesis, T.U. Eindhoven, The Netherlands.
10- Huang, L.X.; Kumar, K.; Mujumdar, A.S., (2003), "A parametric study of the gas flow patterns and drying performance of co-current spray dryer: results of a computational fluid dynamics study", Drying Technolgy, No. 6, Vol. 21, pp. 975.
11- Saleh, S.N., "Prediction of air flow, temperature and humidity patterns in a pilot plant spray dryer", (2010), Nahrain university, College of Engineering Journal (NUCEJ), No.1, Vol. 13, pp.55.
12- Woo, M.W.;Che , L.M.; Daud , W.R.W.; Mujumdar , A.S. ; Chen, X.D., (2012), "Highly swirling transient flows in spray dryers and consequent effect on modeling of particle deposition", Chemical Engineering Research and Design, Vol. 90, pp. 336.
13- Ullum, T.,"Simulation of a spray dryer with rotary atomizer: the appearance of vortex breakdown", (2006), proceedings of the 15th International Drying Symposium, pp.251.
14- Laith Amjad Hameed, (2014), "Simulation and Experimental Work of Air Flow Pattern in a spray Dryer by Using CFD", M.Sc. Thesis, Tikrit University, Iraq.
15- ANSYS Fluent 15 , (2014), Theory Guide, ANSYS Inc.
16- Haung, L.X.; Kumar, K.; Mujumdar, A.S., (2006), " A comparative study of a spray dryer with rotary disc atomizer and pressure nozzle using computational fluid dynamics simulations", Chemical Engineering and Processing, Vol. 45, pp.461.